Supplement of Atmos. Chem. Phys. Discuss., 15, 11763–11797, 2015
http://www.atmos-chem-phys-discuss.net/15/11763/2015/
doi:10.5194/acpd-15-11763-2015-supplement

Atmospheric Chemistry and Physics
Discussions

Supplement of

Relationships between photosynthesis and formaldehyde as a probe of isoprene emission

Y. Zheng et al.

Correspondence to: Y. Zheng (yiqi.zheng@yale.edu)

Supplementary

Meteorological drivers of GPP and HCHOv in NASA ModelE2-YIBs

We apply simulated monthly data of GPP and HCHOv from NASA ModelE2-YIBs in nine model years to investigate their meteorological drivers. Fig. S1 shows the multiple linear regression (MLR) results for monthly mean GPP and HCHOv against T_s, PAR (SW for HCHOv) and P. In the three simulations Y-PS, Y-MEGAN and Y-MEGAN-SM, MLR of GPP results are exactly the same; MLR of HCHOv results only show minor differences. Therefore we only show MLR results using Y-PS isoprene algorithm as a representative in Fig. S1. The standardized partial regression coefficients of GPP and HCHOv associated with T_s, PAR (SW for HCHOv) and P are denoted by GPP_β_T_s, GPP_β_PAR, GPP_β_P and HCHOv_β_T_s, HCHOv_β_SW, HCHOv_β_P. The regionally averaged β-coefficients are summarized in Table S1 including all three simulations.

As in Fig. S1(a), the MLR of simulated GPP reproduces main observational patterns from FLUXNET-GPP successfully but with some non-consistencies: (1) GPP is strongly positively related to T_s in the NH springtime and summertime high-latitudes, and is anticorrelated in tropics and summertime NH mid-latitudes when T_s values approach or exceed the photosynthetic thermal optimum. The model overestimates this anticorrelation with T_s especially in the tropics: in the Amazon simulated GPP_β_T_s = -0.13, -0.18 and -0.41 in MAM, JJA and SON (Table S1); but observational GPP_β_T_s = 0.11, 0.14 and

0.24, respectively (Table 2). This is most probably due to its bias in meteorology: e.g. Amazonian T_s in the model is about 2~3°C higher than in the MERRA reanalysis (Table 1), and is always higher than the thermal optimum 25°C. (2) GPP is overall positively related to PAR, while the simulated negative relationship with PAR in NH high-latitudes might be problematic. (3) The relationship between GPP and precipitation is always positive, especially in the tropics in MAM and SON (in the Amazon GPP_β_P = 0.41, 0.11, and 0.28 in MAM, JJA and SON).

In Fig. S1(b), the MLR of simulated HCHOv shows smoother pattern than observational results of OMI-retrieved HCHO. The covariance of simulated HCHOv with T_s and SW are much stronger than the covariance with P. Simulated HCHOv is strongly positively related to T_s because increasing temperature promotes isoprene emission and oxidation to HCHO, except in some regions with hardly any precursors (e.g. Tibet Plateau and Sahara) where increasing temperature accelerates the chemical destruction of HCHO. The sensitivity to T_s decreases when T_s gets relatively high (e.g. in the tropics and in summertime NH mid-latitudes). Similarly, it’s clear in Fig. S1(b) that light facilitates both HCHO formation and destruction: in most regions HCHOv is negatively related to SW in MAM and SON, and is weakly correlated with SW in JJA. The role of P in influencing HCHOv is much weaker than T_s and SW in NASA ModelE2-YIBs.

Table S1. Regionally averaged MLR β-coefficients with standard deviation for simulated GPP and HCHOv from NASA ModelE2-YIBs in the southeast US, defined as [31 to 35°N; -94 to -79°E] and the Amazon defined as [-15°S to 3°N, -76° to -54°E]. The covariance of GPP with T_s, PAR and precipitation (P) are denoted as GPP_β_T_s, GPP_β_PAR, GPP_β_P; the covariance of HCHOv with T_s, SW and precipitation (P) are denoted as HCHOv_β_T_s, HCHOv_β_SW, HCHOv_β_P. MLR of GPP from the three simulations Y-PS, Y-MEGAN and Y-MEGAN-SM are exactly the same; MLR of HCHOv from the three simulations are listed as (a), (b) and (c) in this table.

Southeast US			
MLR of model GPP			
	GPP_β_T_s	GPP_β_PAR	GPP_β_P
MAM	0.77 ± 0.19	0.18 ± 0.12	0.11 ± 0.09
JJA	-0.36 ± 0.26	0.35 ± 0.14	0.14 ± 0.15
SON	0.39 ± 0.27	0.42 ± 0.17	0.29 ± 0.16
MLR of model HCHOv			
	HCHOv_β_T_s	HCHOv_β_SW	HCHOv_β_P
MAM	(a) 0.76 ± 0.11 (b) 0.77 ± 0.13 (c) 0.75 ± 0.11	(a) 0.20 ± 0.09 (b) 0.16 ± 0.14 (c) 0.20 ± 0.12	(a) -0.05 ± 0.07 (b) -0.09 ± 0.08 (c) -0.07 ± 0.08
JJA	(a) 0.38 ± 0.25 (b) 0.58 ± 0.23	(a) 0.02 ± 0.23 (b) -0.04 ± 0.27	(a) -0.30 ± 0.17 (b) -0.21 ± 0.13

	(c) 0.49 ± 0.23	(c) 0.06 ± 0.24	(c) -0.27 ± 0.16
SON	(a) 0.64 ± 0.15 (b) 0.77 ± 0.25 (c) 0.72 ± 0.19	(a) -0.33 ± 0.16 (b) 0.16 ± 0.22 (c) -0.23 ± 0.17	(a) -0.02 ± 0.09 (b) -0.06 ± 0.13 (c) -0.02 ± 0.11
Amazon			
MLR of model GPP			
	GPP_β_T_s	GPP_β_PAR	GPP_β_P
MAM	-0.13 ± 0.50	0.31 ± 0.31	0.41 ± 0.37
JJA	-0.18 ± 0.57	0.18 ± 0.32	0.11 ± 0.38
SON	-0.41 ± 0.59	0.20 ± 0.22	0.28 ± 0.42
MLR of model HCHOv			
	HCHOv_β_T_s	HCHOv_β_SW	HCHOv_β_P
MAM	(a) 0.30 ± 0.50 (b) 0.42 ± 0.39 (c) 0.39 ± 0.44	(a) -0.05 ± 0.36 (b) -0.12 ± 0.33 (c) -0.14 ± 0.33	(a) 0.39 ± 0.45 (b) 0.20 ± 0.45 (c) 0.18 ± 0.46
JJA	(a) 0.55 ± 0.34 (b) 0.77 ± 0.37 (c) 0.69 ± 0.31	(a) -0.04 ± 0.29 (b) -0.07 ± 0.18 (c) -0.07 ± 0.23	(a) 0.18 ± 0.28 (b) 0.23 ± 0.28 (c) 0.22 ± 0.27
SON	(a) 0.41 ± 0.36 (b) 0.90 ± 0.63 (c) 0.78 ± 0.59	(a) -0.26 ± 0.25 (b) -0.34 ± 0.22 (c) -0.29 ± 0.24	(a) 0.15 ± 0.59 (b) 0.25 ± 0.63 (c) 0.23 ± 0.64

(a) MLR of model GPP

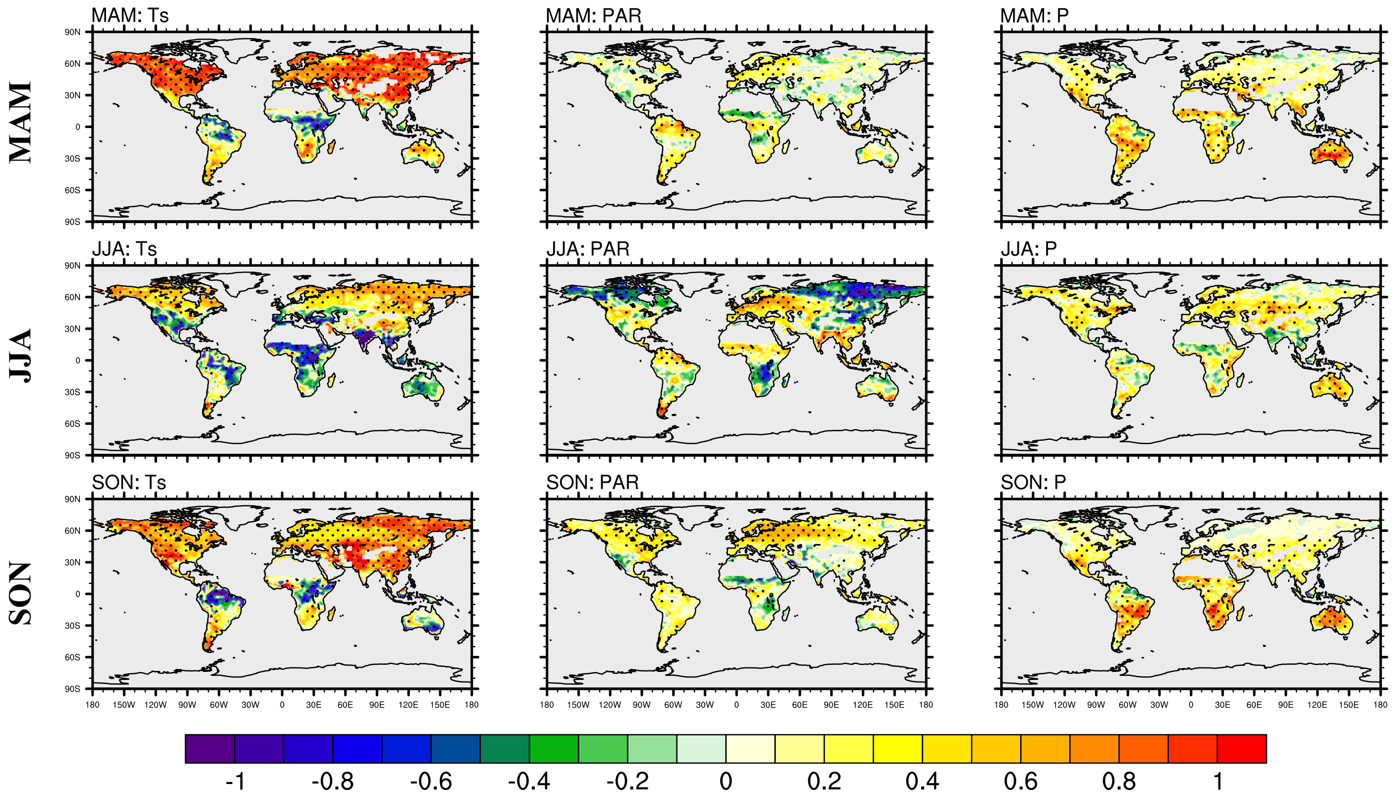

Figure S1(a). The covariance of model GPP in NASA ModelE2-YIBs with monthly mean surface temperature (T_s), photosynthetically active radiation (PAR) and precipitation (P) in MAM (top), JJA (middle) and SON (bottom) from the MLR analysis. MLR is calculated using monthly data in nine model years. Significant regions ($p<0.05$) are shown with dotted shading.

(b) MLR of model HCHOv

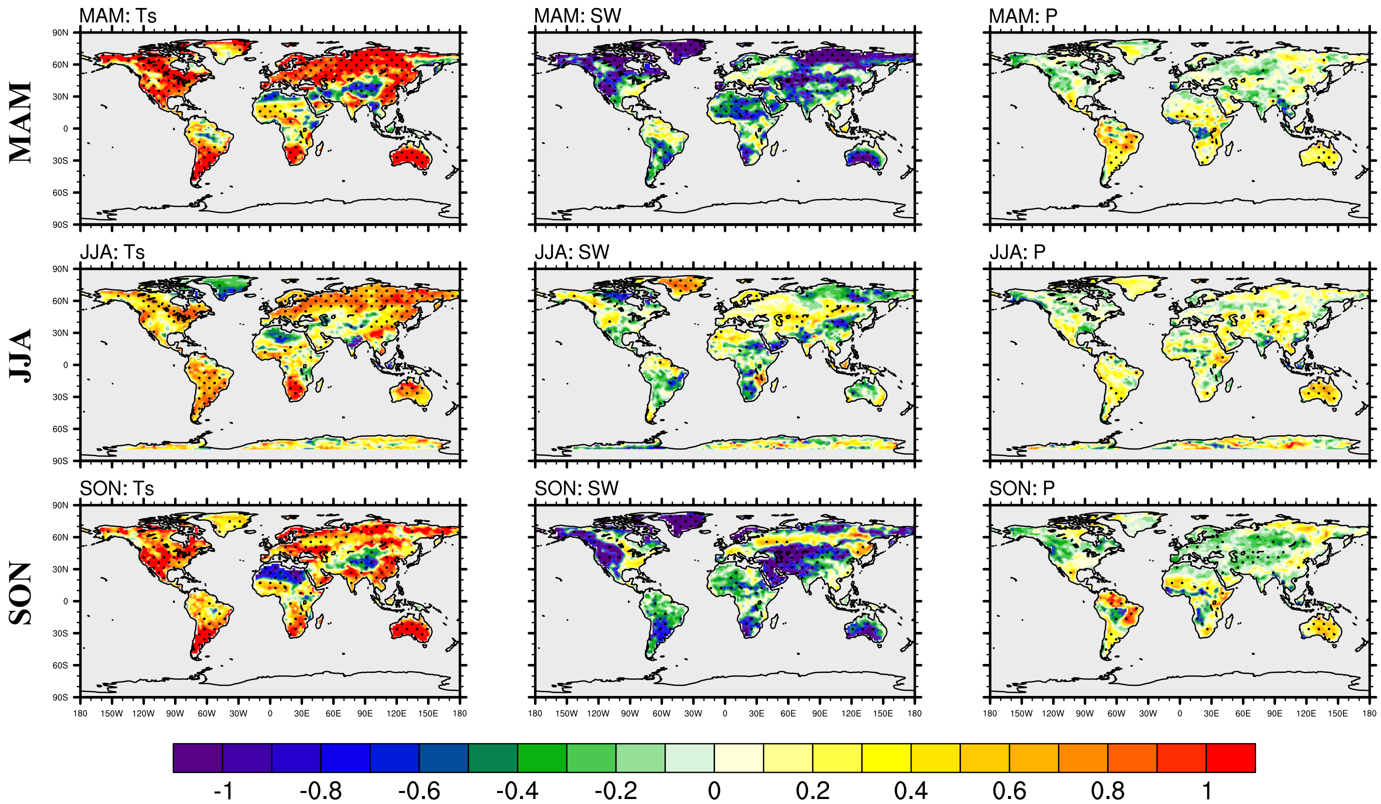

Figure S1(b). The covariance of model HCHOv in NASA ModelE2-YIBs (using Y-PS isoprene algorithm) with monthly mean surface temperature (T_s), downward solar radiation (SW) and precipitation (P) in MAM (top), JJA (middle) and SON (bottom) from the MLR analysis. MLR is calculated using monthly data in nine model years. Significant regions ($p<0.05$) are shown with dotted shading.